Rhizosphere activity in an old-growth forest reacts rapidly to changes in soil moisture and shapes whole-tree carbon allocation

Jobin Joseph[a,1], Decai Gao[a,b,1], Bernhard Backes[c], Corinne Bloch[d], Ivano Brunner[a], Gerd Gleixner[e], Matthias Haeni[a], Henrik Hartmann[e], Günter Hoch[d], Christian Hug[a], Ansgar Kahmen[d], Marco M. Lehmann[a], Mai-He Li[a,b], Jörg Luster[a], Martina Peter[a], Christian Poll[f], Andreas Rigling[a,g], Kaisa A. Rissanen[h], Nadine K. Ruehr[i], Matthias Saurer[a], Marcus Schaub[a], Leonie Schönbeck[a], Benjamin Stern[a], Frank M. Thomas[c], Roland A. Werner[j], Willy Werner[c], Thomas Wohlgemuth[a], Frank Hagedorn[a,1,2], and Arthur Gessler[a,g,1,2]

[a]Swiss Federal Institute for Forest, Snow and Landscape Research, 8903 Birmensdorf, Switzerland; [b]School of Geographical Sciences, Northeast Normal University, 130024 Changchun, China; [c]Geobotany, University of Trier, 54296 Trier, Germany; [d]Physiological Plant Ecology, University of Basel, 4056 Basel, Switzerland; [e]Biogeochemical Processes, Max Planck Institute for Biogeochemistry, 07745 Jena, Germany; [f]Soil Biology, University of Hohenheim, 70599 Stuttgart, Germany; [g]Terrestrial Ecosystems, ETH Zurich, 8092 Zurich, Switzerland; [h]Forest Sciences, University of Helsinki, 00100 Helsinki, Finland; [i]Plant Ecophysiology, Karlsruhe Institute of Technology, 82467 Garmisch-Partenkirchen, Germany; and [j]Agricultural Sciences, ETH Zurich, 8092 Zurich, Switzerland

Edited by James R. Ehleringer, University of Utah, Salt Lake City, UT, and approved August 12, 2020 (received for review July 9, 2020)

Drought alters carbon (C) allocation within trees, thereby impairing tree growth. Recovery of root and leaf functioning and prioritized C supply to sink tissues after drought may compensate for drought-induced reduction of assimilation and growth. It remains unclear if C allocation to sink tissues during and following drought is controlled by altered sink metabolic activities or by the availability of new assimilates. Understanding such mechanisms is required to predict forests' resilience to a changing climate. We investigated the impact of drought and drought release on C allocation in a 100-y-old Scots pine forest. We applied $^{13}CO_2$ pulse labeling to naturally dry control and long-term irrigated trees and tracked the fate of the label in above- and belowground C pools and fluxes. Allocation of new assimilates belowground was ca. 53% lower under nonirrigated conditions. A short rainfall event, which led to a temporary increase in the soil water content (SWC) in the topsoil, strongly increased the amounts of C transported belowground in the nonirrigated plots to values comparable to those in the irrigated plots. This switch in allocation patterns was congruent with a tipping point at around 15% SWC in the response of the respiratory activity of soil microbes. These results indicate that the metabolic sink activity in the rhizosphere and its modulation by soil moisture can drive C allocation within adult trees and ecosystems. Even a subtle increase in soil moisture can lead to a rapid recovery of belowground functions that in turn affects the direction of C transport in trees.

drought | drought release | ^{13}C pulse labeling | sink control

While climate projections predict a higher frequency of extreme weather events, such as hot drought periods (1) but also intermittent heavy rainfall (2), we have limited knowledge on how tree carbon (C) allocation (the distribution of assimilates among tree organs), which is important for whole-tree functioning, is impaired by water restriction (3, 4). Moreover, we lack information on the extent to which C allocation can recover after drought (5, 6). There are several reasons for this knowledge gap: 1) Most experiments on C allocation dynamics have investigated the impact of extreme drought events on trees and ecosystems (7–9) but neglected the more common subtle variations in soil moisture occurring in natural ecosystems. For example, a simulation of the European 2003 drought—assumed to represent an extreme event—in a range of forest ecosystems showed that the soil water reduction was moderate (10) compared with the drought conditions created in most experimental studies on C allocation (e.g., refs. 3 and 11). 2) There are indeed many studies that address small but realistic variations in soil moisture but most of these have solely focused on aboveground responses of tree C relations (12, 13) or integrated whole-ecosystem CO_2 exchange impacts (14, 15) while not taking into account interactions and linkages between shoots and roots and the associated rhizosphere microbiome. For juvenile trees, though, C transfer between shoots, roots, and rhizosphere microbes was found to be crucial for both plant and microbial functioning under stress (9).

Concerning the aboveground–belowground linkage, drought moderately increased C allocation to roots in some studies (16) while reduced allocation was reported in others (17). These inconsistencies are difficult to interpret because the mechanisms that control C allocation within plants and ecosystems are largely unknown; this is a critical knowledge gap, considering that ca. 50% of the energy-demanding processes in the rhizosphere—including roots, mycorrhizal fungi, and bacteria—are fueled by recently assimilated C (18). The mechanisms of C allocation under water stress remain particularly unexplained in mature

Significance

Climate change increases the frequency of drought events and leads to higher variability in precipitation. Drought impairs rhizosphere (root and the root-associated microbiome) functioning in trees and leads to a reduced assimilate supply belowground. It remains unclear if rhizosphere and thus whole-tree functioning can quickly recover after drought release. We show that rhizosphere metabolic activity in previously drought-exposed 100-y-old Scots pine increased in response to subtle soil moisture increases (induced by light rainfall). As a consequence of this activity change, the belowground allocation of new assimilates was immediately stimulated. Even light rainfall events can lead to a fast recovery of rhizosphere functioning and the increased C and energy demand is instantly met by altered whole-tree assimilate allocation.

Author contributions: N.K.R., F.H., and A.G. designed research; J.J., D.G., B.B., C.B., I.B., G.G., H.H., G.H., C.H., M.M.L., M.-H.L., J.L., M.P., C.P., A.R., K.A.R., M. Saurer, M. Schaub, L.S., B.S., F.M.T., R.A.W., W.W., T.W., F.H., and A.G. performed research; J.J., D.G., C.B., I.B., M.H., G.H., M.M.L., J.L., M.P., C.P., K.A.R., M. Saurer, B.S., R.A.W., F.H., and A.G. analyzed data; and J.J., D.G., B.B., C.B., I.B., G.G., M.H., H.H., G.H., C.H., A.K., M.M.L., M.-H.L., J.L., M.P., C.P., A.R., K.A.R., N.K.R., M. Saurer, M. Schaub, L.S., F.M.T., R.A.W., W.W., T.W., F.H., and A.G. wrote the paper.

The authors declare no competing interest.

This article is a PNAS Direct Submission.

[1]J.J., D.G., F.H., and A.G. contributed equally to this work.

[2]To whom correspondence may be addressed. Email: frank.hagedorn@wsl.ch or arthur.gessler@wsl.ch.

This article contains supporting information online at https://www.pnas.org/lookup/suppl/doi:10.1073/pnas.2014084117/-/DCSupplemental.

First published September 21, 2020.

trees and hence in old-growth forests due to a lack of experimental studies, although their understanding is crucial for predicting forest functioning in a drier climate.

The common understanding of the impact of water stress on tree C allocation is that reduced photosynthesis during drought determines the availability of carbohydrates (source control) and can lead, together with impaired phloem transport (19), to reduced C allocation to sink tissues. More recent research indicates control of plant C allocation but also of C assimilation by sink metabolic activity (sink control). In this respect, the belowground sink activity of roots (11) and associated microorganisms (20) seems to play a decisive role. Mild water deficit can increase root growth and metabolic activity to improve water foraging and consequently increases belowground C demand, leading to higher assimilate transport belowground (21). In contrast, drought that exceeds a critical level inhibits belowground metabolism and thus reduces belowground C demand, leading to less C being directed to the rhizosphere (22). Reduced C sink strength can even lead to a down-regulation of photosynthesis (20). In tree saplings, this was assumed to be a result of the acclimation of C assimilation to the reduced sink demand and occurred with a delay of 2 wk after the reduction of the belowground sink activity (11), probably as a result of leaf sucrose accumulation (cf. ref. 23).

Sink control has also been observed directly after drought release: In beech saplings, increased root activity and thus C demand resulted in the prioritized transport of new assimilates belowground, and only in a second step, with a delay of weeks, did photosynthesis readjust to the new conditions and to the higher C demand (11). If the tree C balance after drought release had been under source control, first photosynthesis and only later belowground C transport and sink activity would have increased. So far, experimental studies typically only include young trees and it is unknown if these mechanisms also operate in mature trees in old-growth forests, which store large amounts of reserves that may buffer C allocation.

Rhizosphere microorganisms are an important part of the belowground C sink in ecosystems (24), and the C transfer between forest plants and soil microorganisms is known to be negatively affected by hot droughts (9). It is not fully understood, however, whether drought itself suppresses microbial activity or rather a lower C transfer from plants to the rhizosphere microbiome is the driving force. Moreover, it is not clear if and to what extent rhizosphere microorganisms and their activity are involved in the sink control of whole-tree C allocation.

Taking advantage of a long-term (15-y) precipitation manipulation (irrigation) experiment in a dry inner-Alpine valley in Switzerland (25) and the natural fluctuations of drought and rainfall, we studied the effects of drought and intermittent drought release by a precipitation event on C allocation in a 100-y-old Scots pine forest. We applied $^{13}CO_2$ pulse labeling to 10 mature trees and traced the flux of newly assimilated C from needles into branch, trunk, root, and soil microbial biomass pools and into above- and belowground respiration (Fig. 1). We hypothesized that the soil moisture deficit in the dry nonirrigated plots during periods without rainfall would result in less allocation of recent assimilates belowground and a higher proportion remaining in aboveground tree tissues and fluxes compared with irrigated trees (*SI Appendix*, Fig. S1). We further predicted that short rainfall events, that increase soil moisture above a critical threshold value—allowing increased rhizosphere metabolic activity—would temporarily lead to prioritized transport of assimilates belowground in the normally xeric plots. We expected that rhizosphere sink activity, including the metabolism of roots and associated microorganisms, would control the whole-tree C allocation patterns. As sink control influences photosynthesis with a delay of weeks after changes in sink activity and C allocation patterns (11), we hypothesized that short rainfall events would have only minor effects on C assimilation (*SI Appendix*, Fig. S1).

Results and Discussion

We started a first ^{13}C-labeling campaign at the end of August 2017 after >2 wk of almost no rainfall (<0.9 mm) (*SI Appendix*, Fig. S2*A*), when soil water content in the nonirrigated plots approached values <15% below 2-cm soil depth (*SI Appendix*,

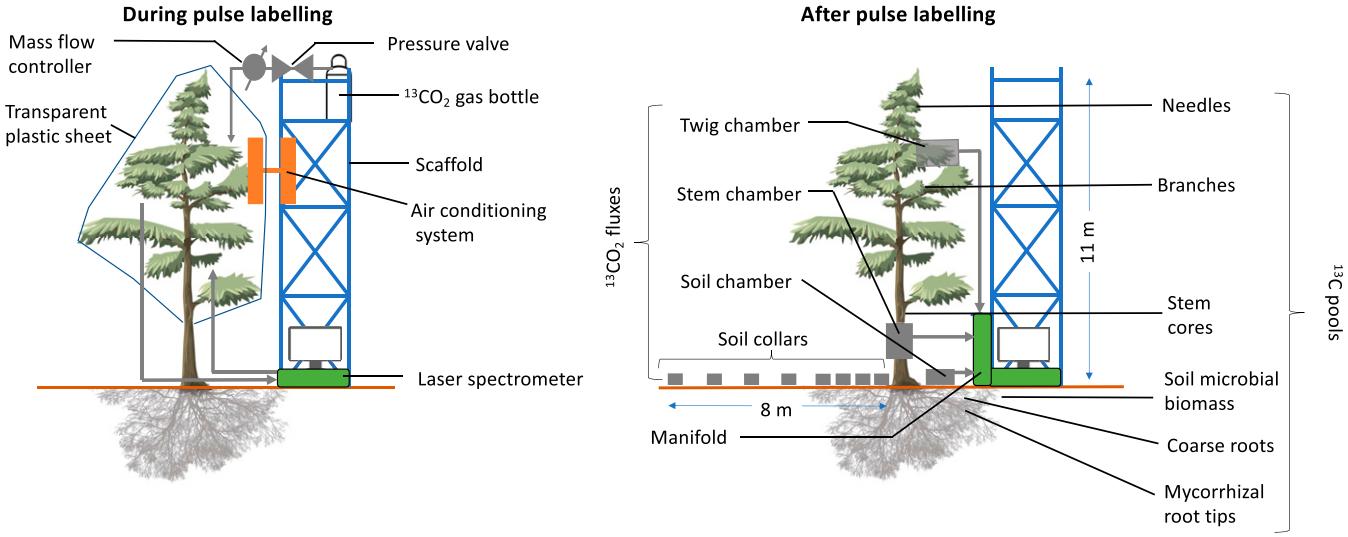

Fig. 1. Setup of the ^{13}C pulse labeling (*Left*) and the tracing of the fate of ^{13}C in respiratory fluxes and plant and soil microbial pools (*Right*). A transparent plastic sheet was erected from scaffolds, enclosing the whole-tree crown to form a labeling chamber. $^{13}CO_2$ was added to the chamber from gas bottles via a mass flow controller. The $^{13}CO_2$ concentration was monitored with LGR CCIA 46d isotope laser spectrometers. The air temperature was adjusted to maintain ambient temperature with an air-conditioning system involving a closed coolant system so that no air exchange between inside and outside the chamber occurred. One branch, stem, and soil chamber per tree were connected via a manifold with automatically controlled solenoid valves to the isotope laser spectrometer. Within a radius of 8 m (along three transects per tree), soil collars were installed to determine the spatiotemporal pattern of soil-respired $^{13}CO_2$ that was measured in the gas samples. Samples of different plant organs and the soil microbial biomass were taken to determine the ^{13}C enrichment at different time points after labeling.

Figs. S2 and S3). Even though leaf water potential was significantly lower ($P = 0.007$) in the dry nonirrigated compared with irrigated plots (Table 1 and *SI Appendix*, Fig. S4), no significant differences were observed for stomatal conductance, transpiration, photosynthetic rate (Table 1 and *SI Appendix*, Fig. S5), or total ^{13}C assimilation during pulse labeling (Table 1 and *SI Appendix*, Table S1). It took approximately 6 d for the ^{13}C assimilated in the canopy of the 10- to 15-m-tall trees to be transferred to the rhizosphere (Fig. 2 *B–E*). Dry conditions in the nonirrigation treatment significantly reduced the allocation of ^{13}C to belowground C sinks, including nonstructural (sugar and starch) and structural C pools in roots, the soil microbial biomass (irrigation effect on ^{13}C allocation to belowground pools: $P = 0.01$; Table 1), and cumulative soil respiratory flux (irrigation effect: $P = 0.009$; Table 1): Thirty days after labeling, the ^{13}C transferred to these belowground sinks was 53% lower in nonirrigated compared with irrigated trees (Fig. 3 and *SI Appendix*, Tab. S2). In contrast to the generally lower transport of new assimilates belowground, mycorrhizal root tips showed comparable ^{13}C incorporation in nonirrigated and irrigated plots (*SI Appendix*, Fig. S6). In forest understory ecosystems it was recently observed that smaller amounts of recent assimilates were transported belowground under drought but that rhizosphere microbes, including mycorrhizal fungi, obtained a relatively larger proportion of these assimilates, thus partially compensating for the change in plant allocation patterns (9). This suggests that plants continue to support the rhizosphere microbiome with recently fixed C during drought to help to sustain its function in water and nutrient acquisition (cf. ref. 26).

Our finding of reduced export to the belowground compartment under drought is in agreement with the longer mean residence time (MRT) of the leaf sugars used as respiratory substrates. The fast-turnover C pool in the canopy of drought-exposed nonirrigated trees had an MRT of 3.8 d, whereas it was only 0.7 d in irrigated trees (*SI Appendix*, Table S3). This range is consistent with values from other studies on pine (27, 28), and comparable increases in MRT as a result of drought have been observed in European beech seedlings (3). The authors of the latter study hypothesized that reduced sink activity, for example in the roots, was not responsible for the higher MRT but rather a higher demand for osmotically active substances in the leaves together with impaired phloem loading (29). More recently, however, an assessment of temporal changes in root and shoot metabolite concentrations and metabolic activity in beech seedlings demonstrated that not only drought but also drought release initially impacted sink activity in the roots, and only with a delay did sink activity feed back on the source organ (11). The reduced sink activity during drought led to reduced leaf phloem loading and increased metabolite accumulation in the leaves and the increased root activity after drought to increased belowground transport but not to an immediate stimulation of photosynthesis.

Our second ^{13}C-labeling application after the short rainfall event (8 mm; *SI Appendix*, Fig. S2*A*) highlights that, in a 100-y-old forest, even subtle but significant changes in soil water availability in the uppermost soil layer (precipitation effect: $P = 0.04$; Table 1) rapidly increased rhizosphere sink activity and C allocation belowground, demonstrating sink control mechanisms acting also in old trees. The rainfall event increased soil water content (SWC) in the uppermost 5 cm of the dry nonirrigated plots to values similar to those in irrigated plots prior to the rainfall (*SI Appendix*, Fig. S3), while SWC in deeper layers (10 and 80 cm) was less affected (*SI Appendix*, Fig. S2 *B* and *C*). This soil moisture increase led to a significant increase in 1) the absolute $^{13}CO_2$ soil respirational flux (Fig. 2 *B* and *C*), and 2) the incorporation of ^{13}C label into the soil microbial (i.e., bacterial and fungal) biomass (Fig. 2 *D* and *E*) in the nonirrigated compared with irrigated plots, resulting in a significant interaction between precipitation and irrigation ($P < 0.05$). The ^{13}C balance calculated for 30 d after labeling showed that relative belowground allocation in trees labeled after the rainfall event was higher in the nonirrigated than in irrigated plots (Fig. 3 and *SI Appendix*, Table S2). Trees in the nonirrigated plots significantly

Table 1. Results of the linear mixed-effects models testing the effects of precipitation, irrigation, and their interaction on soil water content, predawn leaf water potential, gas exchange parameters, total $^{13}CO_2$ taken up, and the relative allocation of ^{13}C to belowground pools and soil respiration

Parameter	Fixed effect	DF	*F* value	*P* value
Soil water content (0 to 5 cm), g $H_2O \cdot g^{-1}$ soil	Precipitation	1,3	11.9	0.040*
	Irrigation	1,3	57.3	0.004**
	Precipitation x irrigation	1,3	2.9	0.18
Leaf water potential, MPa	Irrigation	1,3	25.2	0.007**
Photosynthesis, $\mu mol \cdot m^{-2} \cdot s^{-1}$	Precipitation	1,3	0.05	0.84
	Irrigation	1,3	1.9	0.30
	Precipitation x irrigation	1,3	14.4	0.06
Stomatal conductance, $mmol \cdot m^{-2} \cdot s^{-1}$	Precipitation	1,3	0.13	0.75
	Irrigation	1,3	1.94	0.300
	Precipitation x irrigation	1,3	0.86	0.45
Transpiration, $mmol \cdot m^{-2} \cdot s^{-1}$	Precipitation	1,3	0.18	0.70
	Irrigation	1,3	4.14	0.17
	Precipitation x irrigation	1,3	0.68	0.49
Total $[^{13}C]CO_2$ assimilated, g	Precipitation	1,3	11.4	0.042*
	Irrigation	1,3	2.9	0.19
	Precipitation x irrigation	1,3	0.1	0.76
^{13}C allocation to belowground pools, %	Precipitation	1,3	3.0	0.17
	Irrigation	1,3	13.1	0.01*
	Precipitation x irrigation	1,3	69.2	0.006**
^{13}C allocation to soil respiration, %	Precipitation	1,3	0.13	0.73
	Irrigation	1,3	34.3	0.009**
	Precipitation x irrigation	1,3	11.4	0.04*

Leaf water potential was measured only before the rainfall event (*SI Appendix*, Fig. S4). *$P < 0.05$, **$P < 0.01$. DF, degrees of freedom (numerator DF,denominator DF).

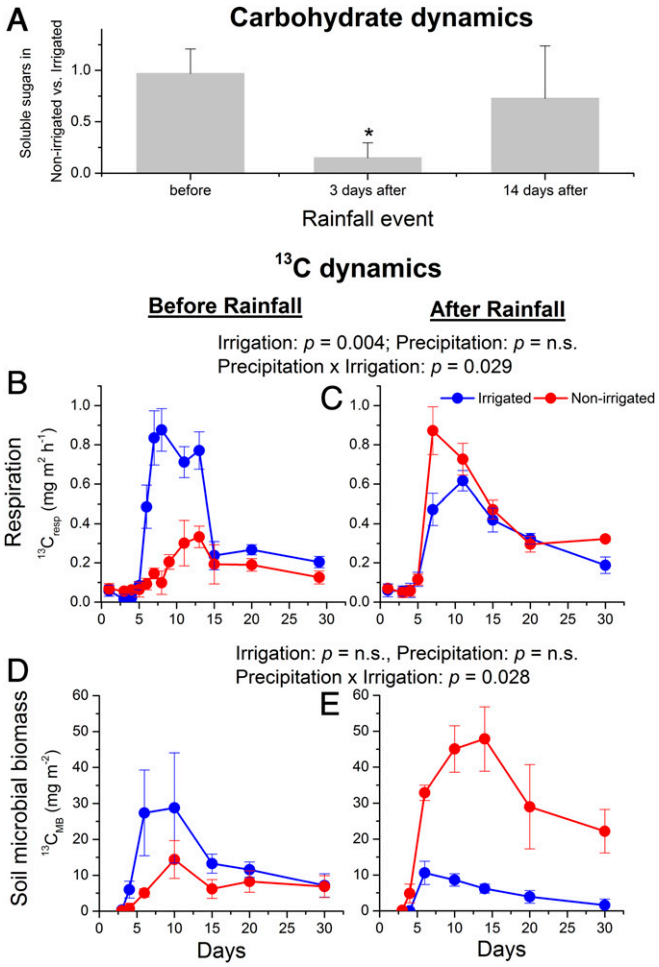

Fig. 2. Dynamics of water-soluble carbohydrates in root tissues and of ^{13}C in soil-respired CO_2 and microbial biomass before and after the rainfall event. (*A*) The ratio of root-soluble sugars between trees from naturally dry nonirrigated and irrigated plots before as well as 3 d and 2 wk after the rainfall event. The data for the time before the rainfall event were taken from ref. 25, where root samples were collected during a dry period in summer. (*B* and *C*) The temporal course of ^{13}C in the soil CO_2 flux in the nonirrigated and irrigated plots after pulse labeling (at $t = 0$ d) before and after the rainfall event. (*D* and *E*) The ^{13}C incorporation into soil microbial biomass (on a m^2 soil surface basis) in the nonirrigated and irrigated plots labeled before or after the rainfall event. Error bars indicate SD in *A* and SE in *B* to *E*. The asterisk in *A* indicates significant differences at $P < 0.05$ according to Student's *t* test ($n = 3$). n.s., not significant.

increased relative allocation to roots and the rhizosphere, while belowground allocation in the irrigated plots remained unaffected by the rainfall event (indicated by a significant irrigation x precipitation interaction: $P = 0.006$ for belowground pools and $P = 0.04$ for soil respiration; Table 1).

To explore the mechanism behind this rapid change in the partitioning of recent assimilates between above- and belowground compartments, we estimated the moisture dependency of microbial soil respiration (and thus microbial activity) from root-free soil adjusted to different soil moisture levels in the laboratory. Results revealed a clear tipping point of microbial respiration at around 15% SWC (Fig. 4*A*). Such soil moisture-dependent tipping points in soil microbial activities have been observed in various other drought studies (30). Total respiratory ^{13}C soil flux (rhizosphere respiration) in the field (Fig. 4*B*) reflecting the use of new assimilates by the rhizosphere showed a similar moisture dependency than microbial activity (Fig. 4*A*). This congruence suggests the existence of a soil moisture-dependent tipping point for the sink activity of the entire root-rhizobiome system increasing the use of new assimilates and thus the allocation to roots and the rhizosphere. Even though the number of pulse-labeled trees was rather low and only one rainfall event was examined (three nonirrigated and three irrigated trees before and two of each treatment after the rainfall event), 61% of the moisture dependency of the ^{13}C flux could be explained by the threshold-type Boltzmann function fitted to microbial respiration in soils without roots (Fig. 4*B*). At the same time, total ^{13}C-label uptake by trees and leaf-level photosynthetic rates did not differ significantly between the treatments (Table 1 and *SI Appendix*, Table S1). Consequently, the root-rhizobiome activity and whole-tree assimilate allocation patterns changed rapidly after a short rainfall event without a change in CO_2 assimilation. These findings indicate that belowground metabolic activity and its modulation by soil moisture drove C allocation and transport within the adult trees and the whole-forest ecosystem.

The reactivation of the rhizosphere sink by intermittent rainfalls likely depends on both rainfall patterns and vertical distribution of the rhizosphere. Our mature pine forest had 60% of its entire fine-root system in the uppermost 10 cm (measured down to 80 cm) (31), which corresponds to other temperate forest ecosystems (32). Fine roots from the uppermost soil layer are physiologically more active and more strongly colonized with mycorrhizal fungi as compared with deeper roots that ensure the water supply of trees during severe droughts (33–35). We thus assume that the observed rewetting of the topsoil affected the largest part of the metabolically active rhizosphere, but in soils with deeper fine-root systems such as Mediterranean forests (36) responses of the rhizosphere sink to intermittent rainfalls might be less pronounced.

In a previous study at the same site (25), we showed that concentrations of soluble sugars in all tree compartments (needles, stems, and roots) were comparable between nonirrigated and irrigated trees in summer and autumn, when soil moisture was clearly lower in the nonirrigated plots. It was concluded that carbohydrate supply and demand were balanced over the long term. Here, we observed a strong and significant depletion of the soluble sugars in the roots in the nonirrigated plots (relative to values in the irrigated plots) shortly after the rainfall event ($P < 0.05$), and only 2 wk later the pool was replenished (Fig. 2*A*). This suggests that despite long-term adjustments of the C balance, short-term fluctuations can occur due to fast increases in belowground metabolic activity (Fig. 4), leading to a transient imbalance of supply and demand. Consequently, the increased C demand explains the higher proportion of new assimilates transported belowground and corroborates the idea of sink control of C allocation. Notably, changes in C allocation driven by the root-rhizobiome system act on very short timescales: Even though the rainfall event occurred shortly after the first ^{13}C labeling, the belowground allocation of ^{13}C remained low in the nonirrigated plots (Fig. 3). Only the new assimilates formed right after the rainfall event were differently distributed, supporting the importance of new assimilates in fueling belowground processes (18) and indicating that the distribution patterns of new assimilates are kept stable after the initial allocation.

Our results provide evidence for adult trees that drought reduces the allocation of recent assimilates belowground. Our findings also demonstrate that mature forest ecosystems in xeric environments can exhibit highly dynamic short-term changes in assimilate distribution: Sudden increases in soil water availability in the uppermost soil layer can result in a boost of belowground metabolic activity and carbohydrate depletion in roots, which in turn lead to strongly increased assimilate transport to the rhizosphere. We acknowledge that we only captured a single recovery event in a single ecosystem and thus we are cautious in

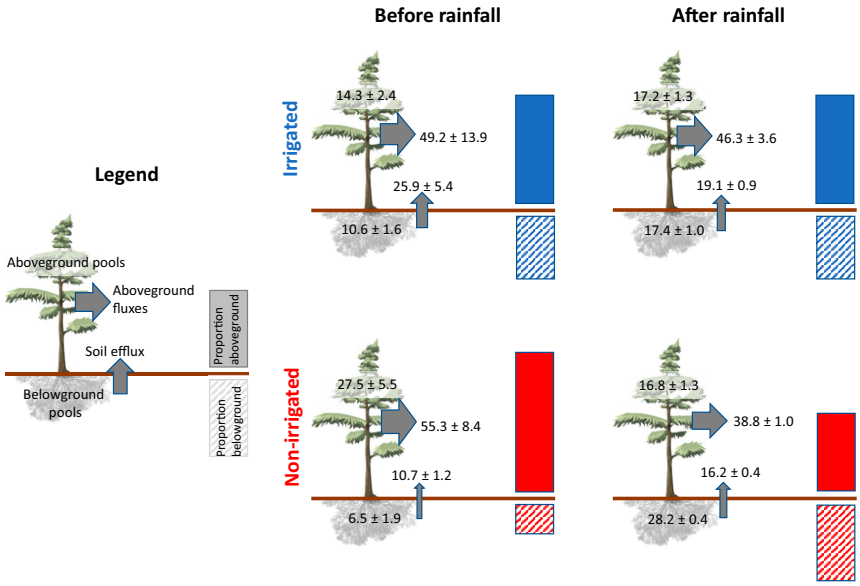

Fig. 3. Relative distribution of the recently assimilated ^{13}C from pulse labeling applied before and after the rainfall event. The percentages of total assimilated ^{13}C recovered in different pools and fluxes, as well as the overall above- and belowground distribution, are shown in irrigated and nonirrigated plots. Aboveground fluxes comprise canopy plus stem respiration, while aboveground biomass pools include structural and nonstructural C from needles, branches, and the stem (for individual values, see *SI Appendix*, Table S2). Belowground pools comprise structural and nonstructural C from roots plus the soil microbial biomass (for individual values, see *SI Appendix*, Table S2). Data shown are integrated fluxes until day 30 after the application of the pulse labeling and the recovery in the pools harvested at day 30. Arrow widths (indicating fluxes) and bars (indicating the overall below- and aboveground distribution) scale proportionally. Aboveground flux data after the rainfall event were not directly measured but calculated as described in *SI Appendix, Methods*. Both the relative allocations of new assimilates to total belowground pools and fluxes and to belowground respiration in particular were significantly affected by the irrigation treatment (belowground pool, $P = 0.01$; soil respiration, $P = 0.009$) but also by the interaction between irrigation treatment and the rainfall event (belowground pool, $P = 0.006$; soil respiration, $P = 0.04$; for detailed statistical information, see Table 1 and *SI Appendix*, Table S2).

extrapolating our results to other forest ecosystems with different species and to droughts and subsequent recovery events of different magnitudes and durations. As a consequence, more experiments on C allocation in various old-growth forest ecosystems under a range of environmental conditions are needed. Our results, however, provide indications that fluctuations in soil water availability in dry sites allow belowground processes to recover fast after rainfall events, and the increased C and energy demand is immediately reflected in changes in whole-tree and ecosystem assimilate allocation patterns. The moisture-sensitive sink strength of the rhizosphere, including roots and the root-rhizobiome system, represents an important but so far overlooked driver of forests' responses to drought and drought release, altering the direction of carbon transport in trees and ultimately modifying physiological acclimation to drought.

Materials and Methods

Experimental Site. The ^{13}C pulse-labeling experiment was carried out with ~100-y-old Scots pine (*Pinus sylvestris* L.) trees growing in a naturally regenerated forest (Pfynwald) in the dry inner-Alpine valley of the river Rhone, one of the driest parts of the European Alps (46° 180 N, 7° 360 E, 615 m above sea level [a.s.l.]). The soil is a shallow 20-cm-thick Pararendzina (37), annual mean temperature is 10.1 °C, and annual precipitation is ca. 600 mm. In the recent past, the forest has been subjected to drought- and heat-induced forest mortality (38). Since 2003 (for 15 y), four plots of 25 × 40 m^2 each have been irrigated at night with 600 $mm \cdot y^{-1}$ between April and October (25), thus doubling the amount of precipitation per year and removing soil water limitation. Four corresponding nonirrigated plots serve as naturally dry controls (for more details, see *SI Appendix, Methods*).

^{13}C Pulse Labeling. In late summer 2017, 10 (five naturally nonirrigated and five irrigated) 100-y-old Scots pine trees were $^{13}CO_2$-labeled (Fig. 1). Three pairs of trees were pulse-labeled during a dry period (little precipitation within >2 wk before pulse labeling) on consecutive days, and another two pairs were labeled immediately after a short rainfall event (*SI Appendix*, Fig. S2). Transparent plastic chambers enclosing the whole crown were erected from scaffolds and temperature and relative humidity were kept at ambient levels using a mobile air-conditioning system (Fig. 1). At each labeling event, two trees, one irrigated and one nonirrigated, were labeled simultaneously. After sealing the chamber, CO_2 with >99 atom% ^{13}C (Cambridge Isotopes) was released into the chamber over a period of 3.5 h, increasing the $^{13}CO_2$ concentration to 1,000 to 1,500 ppm (parts per million), with a $\delta^{13}C$ of up to 250,000 (‰) (measured with an isotope laser spectrometer; LGR CCIA 46d; Los Gatos Research; *SI Appendix*, Figs. S7 and S8). Afterward the chambers were removed, and large industrial blowers set up on the forest floor were used to rapidly remove nonassimilated $^{13}CO_2$.

Measurements of Soil Water Content, Leaf Gas Exchange, and Canopy, Stem, and Soil $^{13}CO_2$ Efflux.

Soil water. Volumetric soil water content at depths of 10 and 80 cm was measured every 15 min across the eight plots of the experimental site using soil moisture sensors (ECH_2O EC-5; Decagon Devices). In addition, soil water content was repeatedly determined gravimetrically at 0- to 2-, 2- to 5-, and 5- to 10-cm depth by sampling soils at 12 locations around each of the pulse-labeled trees, bulking the samples, and drying them at 105 °C.

Gas exchange. Leaf-level gas exchange (transpiration [E], stomatal conductance [g_s], assimilation [A]) was measured with a portable gas exchange measurement device (LI-6400; LI-COR) before and after the rainfall event in the upper third and thus fully sun-exposed part of the canopy. Four trees of each treatment (irrigated and nonirrigated) and needles from three twigs of each tree were measured before and after the rainfall event. The CO_2 concentration inside the cuvette was set to 400 ppm, cuvette temperature to 25 °C, and photosynthetic photon flux density to 1,000 $\mu mol \cdot m^{-2} \cdot s^{-1}$. Relative humidity was adjusted to ambient conditions and flow rate was set to 650 $\mu mol \cdot s^{-1}$. Branch water potential was determined with a Scholander pressure chamber (39) in six trees per treatment (and with three branches per tree) before the rainfall event. Both leaf-level gas exchange and branch water potential were determined around midday.

$^{13}CO_2$ fluxes: high-resolution measurements. For tracking the temporal patterns of ^{13}C allocation, canopy (leaves and branches), stem, and soil $^{13}CO_2$ fluxes of trees labeled before the rainfall event ($n = 6$) were measured with an hourly

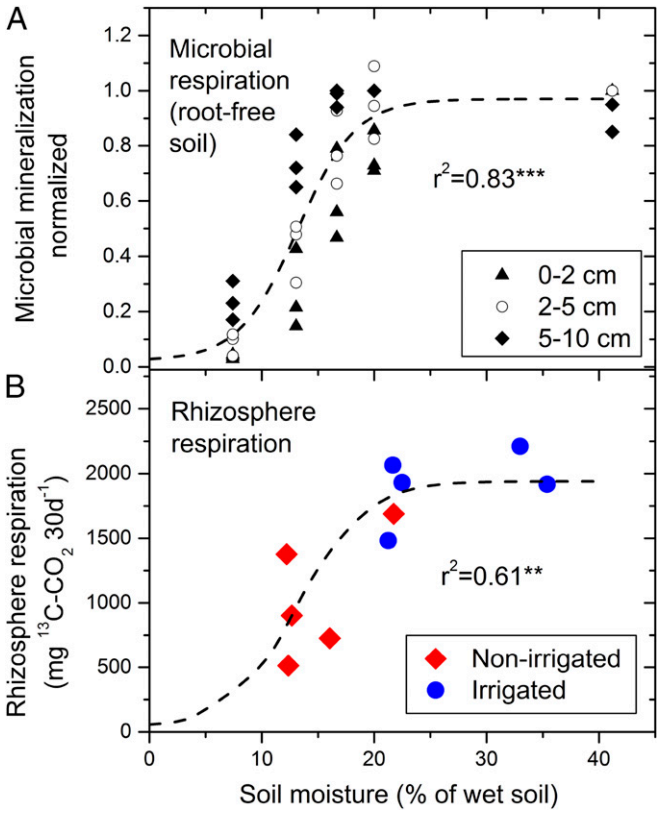

Fig. 4. Effect of soil moisture availability on microbial C mineralization (=heterotrophic respiration) rate (*A*) and on cumulative belowground respiration of recent assimilates (*B*). In *A*, soil microbial respiration was determined in soil samples (excluding roots) from three different depths (0 to 2, 2 to 5, and 5 to 10 cm) at different soil moisture levels adjusted under controlled conditions. In *B*, soil [^{13}C]CO_2 flux cumulated over the 30 d after the pulse labeling is depicted against the soil water content at 2- to 10-cm depth shortly after labeling. Here the variation of the soil moisture is affected by treatment (irrigation vs. nonirrigation), precipitation event, and spatial variability. The dashed line in *A* represents the fit of microbial respiration from root-free soil (normalized to maximal rates) to a Boltzmann equation that was then scaled in *B* to rhizosphere respiration without changing moisture dependencies. r^2 is the coefficient of determination; $^{**}P < 0.01$, $^{***}P < 0.001$.

resolution for 20 consecutive days after pulse labeling (*SI Appendix*, Fig. S9) by coupling three stable isotope laser spectrometers (LGR CCIA 46d; Los Gatos Research) with custom-made automated soil, leaf, and branch chambers designed for gas exchange measurements (40) (Fig. 1). Soil chambers were installed at a distance of 0.5 m from the stem of each tree, stem chambers were attached at the stem approximately 1.5 m aboveground, and branches from the upper third of the canopy were inserted into the canopy chambers. We assumed no strong gradients in light, vapor-pressure deficit, or other environmental conditions within the sparse canopy of the trees at our stand. In a Scots pine stand with a comparable structure no intracanopy gradients in gas exchange were observed (41), and thus we are confident that the branches selected were representative for the whole canopy.

Chambers were programmed to be open during nonmeasurement intervals to avoid CO_2 accumulation and increases in temperature and humidity inside the chamber system. In the measurement mode they were closed, and the respired CO_2 was allowed to accumulate for 5 min when the gas stream was passed to the isotope laser spectrometer. The δ^{13}C value of respired CO_2 was calculated as a two–end-member mixture of ambient and respired CO_2 sampled in the chamber over time (42) and fluxes were determined from the linear CO_2 concentration increase over time and were related to the surface area of the leaves (canopy), stem, or soil. For the ^{13}C mass balance calculation (see below) for canopy respiration fluxes, only measured nighttime CO_2 fluxes and δ^{13}C values were considered, and daytime fluxes were calculated according to the temperature dependency of nighttime fluxes and the actual temperature. Daytime δ^{13}C values were extrapolated from the time course of nighttime values with an exponential decay function.

Laser-based measurements were used for estimating 1) the time-integrated canopy and stem fluxes for the mass balance calculation (see below), and 2) the mean residence time of recent assimilates in the canopy, stem, and soil (*SI Appendix*, Table S3). Exponential decay models were fitted in the phase of label decrease according to ref. 27 and two labile C pools (i.e., soluble sugars and starch) with different MRT values were assumed.

$^{13}CO_2$ fluxes: low-resolution measurements. For quantifying soil ^{13}C fluxes from the entire rhizosphere of each of the 10 pulse-labeled trees (six trees before the precipitation and four trees afterward), we installed soil collars of 10-cm diameter along three transects at distances of 0.5, 1.0, 1.5, 2.0, 3.0, 4.0, 6.0, and 8.0 m from the tree stems. Soil respiration (R_S) was measured up to a daily resolution with an LI-8100A soil CO_2 flux system with an LI-8100-102 survey chamber (LI-COR) placed on the soil collars over 30 d following pulse labeling. For measuring δ^{13}C values of soil-respired CO_2, the collars were closed with lids and gas samples were taken with syringes after 15 to 20 min. In addition, ambient air close to the soil surface was collected during each sampling period. In gas samples, the δ^{13}C values and the CO_2 concentration were analyzed with a GasBench II (modified according to ref. 43) coupled to a Delta Plus^{XP} isotope ratio mass spectrometer (IRMS) (Thermo Finnigan). The δ^{13}C value of the respired CO_2 was calculated as a two–end-member mixture of ambient and respired CO_2 sampled in the chamber after 15 to 20 min (42).

The low-resolution soil fluxes were used to estimate the soil ^{13}C fluxes integrated over time and space for each of the pulse-labeled trees (see below).

Moisture Dependency of Microbial Soil Respiration. The moisture dependency of heterotrophic soil respiration was determined for 20 g of root-free soil samples from 0- to 2-, 2- to 5-, and 5- to 10-cm depth, which was first dried at room temperature and then rewetted to the desired water content ($n = 6$ per moisture content). Carbon mineralization was measured in gas-tight glass jars of 500-mL volume, equipped with a rubber septum opening through which 8 mL of gas samples was extracted after 24, 48, 72, and 96 h. These samples were injected into preevacuated 4-mL Exetainers and analyzed for CO_2 concentration by gas chromatography (model 7890; Agilent Technologies).

Determination of ^{13}C Recovery in Above- and Belowground Pools.

Sampling and preprocessing. Needle (combined current and previous year's cohorts) and branch samples were collected in the upper third of the canopy 1 h before pulse labeling, directly after labeling (0 h), and until 30 d after labeling (cf. *SI Appendix*, Figs. S10 and S11). The needles were removed from the branches, transferred into paper bags, microwaved to denature all enzymes, and then oven-dried. The branch material was stored in Exetainers in liquid nitrogen and later oven-dried. Stem wood samples plus stem phloem were taken 10 and 30 d after pulse labeling (*SI Appendix*, Figs. S10 and S11). For stem samples, 10-mm-increment cores were taken with an increment borer (Haglöf Sweden) at three locations in a 120° angle around the stem at breast height at each sampling time point. The core samples were transferred into Exetainers and immediately stored at −20 °C. After drying, the outer 30 tree rings and the phloem were used for further analysis. For root sampling, coarse roots were traced from their insertion point into the stem, excavated from the soil, microwaved, oven-dried, and homogenized. Water-soluble compounds (WSCs) and starch were extracted from subsamples of all tree tissues (*SI Appendix, Methods*). To assess mycorrhizal root tips, three soil cores with a diameter of 2 cm were randomly sampled from the upper 0 to 10 cm of the soil [the main rooting horizon (31)] in the immediate vicinity of each tree 0, 7, and 14 d after labeling, and the samples were pooled per tree. Vital mycorrhizal root tips were immediately collected from the soil cores under a stereomicroscope and kept at −70 °C until processing. All bulk tree tissue samples (needles, wood, roots, mycorrhizal root tips) were ground to a fine powder after drying at 80 °C, using a steel ball mill (MM 400; Retsch), for further analysis. For the assessment of C concentrations and δ^{13}C in the bulk organic matter of tree tissues, starch, and WSCs, ca. 0.6 mg of the homogenized and dried material was weighed into tin capsules for further isotope analysis (*SI Appendix, Methods*). To quantify soil microbial biomass, 12 soil cores of 2-cm diameter were sampled within a 1-m distance of each tree and bulked. All roots were removed from the soil, and the samples were then immediately frozen and later analyzed for soil microbial biomass using the chloroform fumigation extraction method. Both the concentration and isotopic signature of extracted organic C from nonfumigated and fumigated samples were determined by oxidizing extractable C to CO_2 (44) and measuring the $^{13}CO_2$ with an IRMS (GasBench II coupled to a Delta V Plus;

Thermo Finnigan) and calculated as described previously assuming a conversion factor of 0.45 (45).

Soluble Sugars in Roots. Concentrations of soluble sugars in roots (Fig. 2*A*) were determined according to ref. 46 as described in detail by ref. 25.

^{13}C Mass Balance Estimation. The amount of ^{13}C taken up by the trees (calculated based on the amount of 99% [^{13}C]CO_2 supplied to the pulse-labeling chamber from the gas cylinder; *SI Appendix*, Table S1) and recovered in the different tree pools and soil microbial biomass and the CO_2 released from branches, stem, and soil were used for a ^{13}C mass balance estimation of individual trees and their related rhizosphere. To assess the total ^{13}C enrichment in the tree pools as a result of labeling, total biomass (g) of the different plant compartments (needles, branches, stem, and roots) was calculated for each tree from allometric functions specific for *P. sylvestris* using tree height and diameter at breast height (DBH) as input parameters (47). In a next step, total C of each biomass pool (C_{pool}; g) was calculated by multiplying the biomass by the specific C content (%) of the pool as determined by the isotope measurements. We performed these calculations separately for bulk C and for nonstructural C (NSC; starch plus WSCs). From the difference between bulk C and NSC, we computed the structural C pool (SC) (*SI Appendix*, Table S2). The C pool of the microbial biomass (0- to 10-cm depths) was estimated by multiplying the microbial biomass by the mass of soil on an area base using measured soil bulk densities. ^{13}C excess, namely the ^{13}C enrichment due to labeling expressed in atom% (*SI Appendix, Methods*) (3) 30 d after the pulse labeling, was multiplied by the C pools of tree and microbial biomass. For the scaling of the ^{13}C excess of the microbial biomass to the circular area around each tree, we linked the ^{13}C excess to the decline of soil-respired $^{13}CO_2$ with distance from the stems. The CO_2 flux rates from the canopy and stem (hourly resolution) were multiplied by the ^{13}C excess and the surface area and integrated over the 30 d after the pulse labeling (*SI Appendix, Methods*). Needle area was determined from the needle mass obtained from tree allometric functions (47) and the specific leaf area was determined for every tree and we assumed gas exchange in the canopy chamber to be representative of gas exchange of the whole canopy. Stem area was determined from DBH and tree height assuming the stem to be a truncated cone with the upper diameter being 5% of DBH. For estimating soil $^{13}CO_2$ flux from the entire rhizosphere of each tree, we interpolated linearly between the fluxes from adjacent soil collars placed at various distances from the tree stems (Fig. 1) measured at daily resolution and integrated them over time. ^{13}C in pools and fluxes was related to the ^{13}C applied during pulse labeling to obtain recovery rates (*SI Appendix, Methods*), and the relative allocation to different pools and fluxes was calculated (Fig. 3 and *SI Appendix, Methods* and Table S2).

Statistical Analysis. Data were analyzed by fitting linear mixed-effects models with maximum likelihood using the lme function in the nlme package (R version 3.1.2). For the entire study period, treatment (irrigated vs. nonirrigated) and date of measurement (before and after the precipitation event) were used as fixed effects in the models and individual tree was included as a random effect. The corAR1 function in the nlme package was included in the models to account for repeated measurements with a first-order autoregressive covariate structure. In all final models, the dependent variables were log- or square root-transformed to achieve normality and homoscedasticity of the residuals.

Data Availability. All study data are included in the article and *SI Appendix*.

ACKNOWLEDGMENTS. This work was funded by the Swiss National Science Foundation under Contracts 31003A_159866 and 310030_189109 (to A.G.) and Sino-Swiss Science and Technology Cooperation (EG 09-122016) (to D.G. and F.H.).

1. C. D. Allen, D. D. Breshears, N. G. McDowell, On underestimation of global vulnerability to tree mortality and forest die-off from hotter drought in the Anthropocene. *Ecosphere* **6**, 129 (2015).
2. Intergovernmental Panel on Climate Change, *Climate Change 2013: The Physical Science Basis. Contribution of Working Group I to the Fifth Assessment Report of the Intergovernmental Panel on Climate Change*, (Cambridge University Press, Cambridge, UK, 2013).
3. N. K. Ruehr *et al*., Drought effects on allocation of recent carbon: From beech leaves to soil CO_2 efflux. *New Phytol.* **184**, 950–961 (2009).
4. H. Hartmann, N. G. McDowell, S. Trumbore, Allocation to carbon storage pools in Norway spruce saplings under drought and low CO_2. *Tree Physiol.* **35**, 243–252 (2015).
5. L. Galiano *et al*., The fate of recently fixed carbon after drought release: Towards unravelling C storage regulation in *Tilia platyphyllos* and *Pinus sylvestris*. *Plant Cell Environ.* **40**, 1711–1724 (2017).
6. A. T. Trugman *et al*., Tree carbon allocation explains forest drought-kill and recovery patterns. *Ecol. Lett.* **21**, 1552–1560 (2018).
7. C. E. Doughty *et al*., Drought impact on forest carbon dynamics and fluxes in Amazonia. *Nature* **519**, 78–82 (2015).
8. H. Aaltonen, A. Lindén, J. Heinonsalo, C. Biasi, J. Pumpanen, Effects of prolonged drought stress on Scots pine seedling carbon allocation. *Tree Physiol.* **37**, 418–427 (2017).
9. I. von Rein *et al*., Forest understory plant and soil microbial response to an experimentally induced drought and heat-pulse event: The importance of maintaining the continuum. *Glob. Change Biol.* **22**, 2861–2874 (2016).
10. K. Felsmann *et al*., Responses of the structure and function of the understory plant communities to precipitation reduction across forest ecosystems in Germany. *Ann. For. Sci.* **75**, 3 (2017).
11. F. Hagedorn *et al*., Recovery of trees from drought depends on belowground sink control. *Nat. Plants* **2**, 16111 (2016).
12. R. Zweifel, L. Zimmermann, F. Zeugin, D. M. Newbery, Intra-annual radial growth and water relations of trees: Implications towards a growth mechanism. *J. Exp. Bot.* **57**, 1445–1459 (2006).
13. J. B. Xia, Z. G. Zhao, J. K. Sun, J. T. Liu, Y. Y. Zhao, Response of stem sap flow and leaf photosynthesis in *Tamarix chinensis* to soil moisture in the Yellow River Delta, China. *Photosynthetica* **55**, 368–377 (2017).
14. S. Greco, D. D. Baldocchi, Seasonal variations of CO_2 and water vapour exchange rates over a temperate deciduous forest. *Glob. Change Biol.* **2**, 183–197 (1996).
15. K. Pilegaard, P. Hummelshøj, N. O. Jensen, Z. Chen, Two years of continuous CO_2 eddy-flux measurements over a Danish beech forest. *Agric. For. Meteorol.* **107**, 29–41 (2001).
16. H. Poorter *et al*., Biomass allocation to leaves, stems and roots: Meta-analyses of interspecific variation and environmental control. *New Phytol.* **193**, 30–50 (2012).
17. I. C. Meier, C. Leuschner, Genotypic variation and phenotypic plasticity in the drought response of fine roots of European beech. *Tree Physiol.* **28**, 297–309 (2008).
18. P. Högberg *et al*., Large-scale forest girdling shows that current photosynthesis drives soil respiration. *Nature* **411**, 789–792 (2001).
19. A. Sala, F. Piper, G. Hoch, Physiological mechanisms of drought-induced tree mortality are far from being resolved. *New Phytol.* **186**, 274–281 (2010).
20. M. E. Gavito, I. Jakobsen, T. N. Mikkelsen, F. Mora, Direct evidence for modulation of photosynthesis by an arbuscular mycorrhiza-induced carbon sink strength. *New Phytol.* **223**, 896–907 (2019).
21. R. Hommel *et al*., Impact of interspecific competition and drought on the allocation of new assimilates in trees. *Plant Biol. (Stuttg.)* **18**, 785–796 (2016).
22. C. Körner, Paradigm shift in plant growth control. *Curr. Opin. Plant Biol.* **25**, 107–114 (2015).
23. D. Fabre *et al*., Is triose phosphate utilization involved in the feedback inhibition of photosynthesis in rice under conditions of sink limitation? *J. Exp. Bot.* **70**, 5773–5785 (2019).
24. R. D. Bardgett, W. D. Bowman, R. Kaufmann, S. K. Schmidt, A temporal approach to linking aboveground and belowground ecology. *Trends Ecol. Evol. (Amst.)* **20**, 634–641 (2005).
25. L. Schönbeck *et al*., Homeostatic levels of nonstructural carbohydrates after 13 yr of drought and irrigation in *Pinus sylvestris*. *New Phytol.* **219**, 1314–1324 (2018).
26. E. George, H. Marschner, Nutrient and water uptake by roots of forest trees. *Z. Pflanz. Bodenkunde* **159**, 11–21 (1996).
27. D. Epron *et al*., Pulse-labelling trees to study carbon allocation dynamics: A review of methods, current knowledge and future prospects. *Tree Physiol.* **32**, 776–798 (2012).
28. D. Desalme *et al*., Seasonal variations drive short-term dynamics and partitioning of recently assimilated carbon in the foliage of adult beech and pine. *New Phytol.* **213**, 140–153 (2017).
29. S. Sevanto, Phloem transport and drought. *J. Exp. Bot.* **65**, 1751–1759 (2014).
30. S. Manzoni, J. P. Schimel, A. Porporato, Responses of soil microbial communities to water stress: Results from a meta-analysis. *Ecology* **93**, 930–938 (2012).
31. I. Brunner, C. Herzog, L. Galiano, A. Gessler, Plasticity of fine-root traits under long-term irrigation of a water-limited Scots pine forest. *Front. Plant Sci.* **10**, 701 (2019).
32. L. Finér, M. Ohashi, K. Noguchi, Y. Hirano, Factors causing variation in fine root biomass in forest ecosystems. *For. Ecol. Manage.* **261**, 265–277 (2011).
33. I. Brunner, C. Herzog, M. A. Dawes, M. Arend, C. Sperisen, How tree roots respond to drought. *Front. Plant Sci.* **6**, 547 (2015).
34. A. Carteron, M. Beigas, S. Joly, B. L. Turner, E. Laliberté, Temperate forests dominated by arbuscular or ectomycorrhizal fungi are characterized by strong shifts from saprotrophic to mycorrhizal fungi with increasing soil depth. *Microb. Ecol.*, 10.1007/s00248-020-01540-7 (2020).
35. A. Germon, J.-P. Laclau, A. Robin, C. Jourdan, Tamm Review: Deep fine roots in forest ecosystems: Why dig deeper? *For. Ecol. Manage.* **466**, 118135 (2020).
36. B. López, S. Sabaté, C. A. Gracia, Vertical distribution of fine root density, length density, area index and mean diameter in a *Quercus ilex* forest. *Tree Physiol.* **21**, 555–560 (2001).

37. I. Brunner *et al*., Morphological and physiological responses of Scots pine fine roots to water supply in a dry climatic region in Switzerland. *Tree Physiol.* **29**, 541–550 (2009).
38. A. Rigling *et al*., Driving factors of a vegetation shift from Scots pine to pubescent oak in dry Alpine forests. *Glob. Change Biol.* **19**, 229–240 (2013).
39. P. F. Scholander, E. D. Bradstreet, E. A. Hemmingsen, H. T. Hammel, Sap pressure in vascular plants: Negative hydrostatic pressure can be measured in plants. *Science* **148**, 339–346 (1965).
40. I. Bamberger *et al*., Isoprene emission and photosynthesis during heatwaves and drought in black locust. *Biogeosciences* **14**, 3649–3667 (2017).
41. E. Brandes *et al*., Short-term variation in the isotopic composition of organic matter allocated from the leaves to the stem of *Pinus sylvestris*: Effects of photosynthetic and postphotosynthetic carbon isotope fractionation. *Glob. Change Biol.* **12**, 1922–1939 (2006).
42. J. A. Subke *et al*., Feedback interactions between needle litter decomposition and rhizosphere activity. *Oecologia* **139**, 551–559 (2004).
43. M. J. Zeeman *et al*., Optimization of automated gas sample collection and isotope ratio mass spectrometric analysis of δ(13)C of CO(2) in air. *Rapid Commun. Mass Spectrom.* **22**, 3883–3892 (2008).
44. S. Q. Lang, S. M. Bernasconi, G. L. Früh-Green, Stable isotope analysis of organic carbon in small (μg C) samples and dissolved organic matter using a GasBench preparation device. *Rapid Commun. Mass Spectrom.* **26**, 9–16 (2012).
45. P. Högberg *et al*., High temporal resolution tracing of photosynthate carbon from the tree canopy to forest soil microorganisms. *New Phytol.* **177**, 220–228 (2008).
46. G. Hoch, A. Richter, C. Körner, Non-structural carbon compounds in temperate forest trees. *Plant Cell Environ.* **26**, 1067–1081 (2003).
47. D. I. Forrester *et al*., Generalized biomass and leaf area allometric equations for European tree species incorporating stand structure, tree age and climate. *For. Ecol. Manage.* **396**, 160–175 (2017).